To appear in the *SREW Proceedings*, 2000.

Geomagnetic and solar wind parameters to predict the relativistic electron fluxes in the outer radiation belt

Paul Bühler, Laurent Desorgher, Alex Zehnder,
Paul Scherrer Institute, Laboratory for Astrophysics, 5232 Villigen, PSI, Switzerland

Michel Kruglanski, Bart Quaghebeur
Belgian Institute for Space Aeronomy, 1180 Brussels, Belgium

Eamonn Daly
ESTEC, NL-2200 AG Noordwijk, The Netherlands

Abstract

The relativistic electron fluxes of the outer radiation belt are subject to strong temporal variations. In order to find a simple model describing these variations we studied the linear correlation with various geomagnetic and solar wind parameters as function of the magnetic L-shell and the length of period over which the parameters were averaged. We find that the average time giving the best correlation is a function of L and typically around 20 days at $L = 4.5\ R_E$, decreasing to around 5 days at $L = 6.6\ R_E$. In the heart of the belt AP gives the best correlations whereas at Geostationary Orbit best correlations are found with the solar wind speed. Corrections for Dst effect, semiannual modulation of the solar wind - magnetosphere coupling and linear combinations of parameters were tested to improve the correlation coefficients. Best fitting models use a linear combination of eighteen day averaged AP and three day averaged solar wind speed and include a correction for Dst effect.

1. Introduction

The energetic electrons trapped in the earth outer radiation belt form a particular hazard to spacecrafts. Whereas the lower energetic electrons are stopped in the surface material of a satellite and cause surface charging, the higher energetic particles can penetrate and lead to internal charging. The following discharging then can cause damage in sensitive devices [*Wrenn and Smith,* 1996]. In addition the accumulated radiation dose leads to a continuous degradation of instrument performance.

One of the characteristics of the trapped relativistic electron population is its dynamism. The observed fluxes vary on various time scales, from fractions of a day to the solar cycle period, over several orders of magnitude. The variations are driven by the solar wind and interplanetary magnetic field, IMF [*Paulikas and Blake,* 1979]. However, the detailed mechanism is not fully understood yet and subject of active debate [*Blake et al.,* 1997; *Baker et al.,* 1998; *Li et al.,* 1999]

The NASA model AE8 [*Vette,* 1991], which was build with data from the 1960/70 is still used as the quasi standard for the characterization of the space environment. There are two versions, one for solar minimum and one for solar maximum conditions. But each of these models is static. They are supposed to predict long-term averages and can not account for the short-term variations.

In order to improve the situation attempts have been made to use the solar wind, IMF, and geomagnetic indices to describe the electron flux variations. Most of the studies have been focused on the Geostationary Orbit, GEO because of the availability of long term electron data sets at this orbit [*Nagai,* 1988; *Baker et al.,* 1990; *Koons et al.,* 1994]. Data from the CRRES satellite in a geostationary transfer orbit, GTO were used to build a number of models for the entire outer radiation belt zone under different geomagnetic activity conditions which are known as CRRESELE models [*Brautigam and Bell,* 1995]. As sorting parameter, AP_{15} was used, the fifteen day average of AP and it shows that generally the model fluxes increase over the entire outer belt with AP_{15}. In these models the same dependence on AP_{15} is used for all L-values.

We used data from the Radiation Environment Monitor, REM [*Bühler et al.,* 1996] aboard the UK-satellite Strv-1b to investigate possible improvements of the scheme applied for the CRRES data. Strv-1b was launched in June 1994 and was operated until September 1998. It was in a GTO with 7° inclination, thus an orbit similar to CRRES. In this paper we especially address the questions

1. is AP the best sorting parameter ?
2. is 15 days the optimum average time ?
3. does one need to use different sorting parameters/average times at different L-values?

2. Method and data

In order to address these questions we calculated linear correlation coefficients between the logarithm of the 1 MeV electron fluxes, $log(f_e(t,L))$ and different averages of various geomagnetic/solar-wind parameters. The periods over which the parameters were averaged are defined by a lag time and an average time. In the following a parameter $\mathcal{P}$, averaged over t_{avg} days with a lag of t_{lag} days is denoted by $\mathcal{P}_{t_{avg},t_{lag}}(t)$.

$$\mathcal{P}_{t_{avg},t_{lag}}(t) = \overline{\mathcal{P}(\tau)}\Big|_{\tau\geq(t-t_{avg}-t_{lag})}^{\tau\leq(t-t_{lag})} \qquad (1)$$

The correlation coefficient between $log(f_e(t,L))$ and $\mathcal{P}_{t_{avg},1}(t)$ is denoted by $cc_{\mathcal{P}}(L,t_{avg})$.

We investigated the correlation as function of t_{avg} and L. t_{lag} was kept fixed at the value of 1 day.

2.1. Data

We used 1 MeV electron data measured with REM during 1995, different geomagnetic indices from NGDC [*NGDC*], and solar wind and interplanetary geomagnetic field data from instruments aboard the WIND satellite [*WIND*]. The left most column in table 1 contains the investigated parameters. Most of them which contain solar wind and IMF measurements are cited in *Gonzales et al.* [1994] which contains a summary of solar wind - magnetosphere coupling functions used in the past for different purposes. Detailed references are given there. table 1

In figure 1 the REM 1 MeV electron fluxes at a) $L = 4.5$ and b) $L = 6.6$ R_E are plotted versus time for 1995. The time series are characterized by repeated enhancements and decays. Although the maxima and minima at both locations occur closely simultaneously there are significant differences between the two curves. At $L = 6.6$ R_E the relative flux variations figure 1 are larger than at $L = 4.5\ R_E$ and the characteristic timescales, especially the decay times, are obviously shorter. The plotted curves suggest, that there is indeed an L-dependence of the temporal variations and that an average of 15 days may not be optimum at all L-values. This is further supported by the fact, that $cc_{AP}(4.5, 15)$ is 0.74, whereas $cc_{AP}(6.6, 15)$ is only 0.32.

3. Correlations

table 2

figure 2

For each of the parameters listed in table 2 we calculated $cc_{\mathcal{P}}$ for a number of L-bins and t_{avg} values. As an example we show in figure 2 the resulting L-t_{avg}-map of cc_{AP} and $cc_{V_{sw}}$. Panels a) and c) show grayscale maps of the correlation coefficients as function of L and t_{avg}. The black dots mark the positions where for a given L-bin the correlation coefficient is maximum. The subpanels below show the correlation coefficient at these positions as function of L.

The observed L-dependence of $t_{avg,AP,best}$ and $t_{avg,V_{sw},best}$ is typical for most of the investigated parameters. Above $L \approx 5\ R_E$ the best fitting average time is around 3 to 5 days and increases below this limit with decreasing L.

In panels b) and d) of figure 2 the t_{avg}-dependence of the correlation coefficients with $AP_{t_{avg},1}$ and $(V_{sw})_{t_{avg},1}$ at $L = 4.5$ (diamonds) and 6.6 R_E (asterisks) are shown. Whereas at $L = 4.5\ R_E$ the correlation coefficient has a broad maximum around 15 to 20 days, there are two humps at $L = 6.6\ R_E$, one centered around 3 to 5 days and one around 20 days. Also this behaviour is typical for most of the investigated parameters.

For each parameter and L-bin we determined the average time $t_{avg,\mathcal{P},best}(L)$ which yields the higest correlation coefficient $cc_{\mathcal{P},best}(L) = cc_{\mathcal{P}}(L, t_{avg,\mathcal{P},best}(L))$. The $t_{avg,\mathcal{P},best}$ and corresponding $cc_{\mathcal{P},best}(L)$ at $L =$ 4.5 and 6.6 R_E are listed in table 1. There are several points to note:

- At $L = 4.5\ R_E$ the best correlation is found with $AP_{18,1}$. However, the maximum in the correlation versus t_{avg} curve is broad and practically flat between 15 and 20 days. $AP_{15,1}$, as used for the CRRESELE models seems to be a good sorting parameter in the heart of the radiation belt.
- At $L = 6.6\ R_E$ the best correlation is found with $(V_{sw})_{3,1}$. The maximum in the correlation versus t_{avg} curve is rather sharp and peaks at 3 days. $(V_{sw})_{3,1}$ gives here a significantly better correlation than $AP_{15,1}$.
- The averaging time, for which the correlation is maximum, is a function of L. Typically $t_{avg,best}$ is small (few days) at large L and increases below $L \approx$ 5.0 R_E. Exceptions are $V_{sw}B_{imf,z}$, $V_{sw}^2 B_{imf,z}$, and $(\rho V_{sw}^2)^{-1/3} V_{sw} B_{imf,t}^2 sin^4(\Theta/2)$, for which anyhow the correlations are poor at all (L,t_{avg})-values.
- At $L = 6.6\ R_E$ the correlation coefficient versus t_{avg} curves of AP, V_{sw}, and most of the other parameter functions have secondary peaks around $t_{avg,best}$ + 27 days, indicating the influence of recurrent fast solar wind streams.
- At GEO the correlations of all of the parameter functions have a more or less pronounced secondary peak around 20 days, which is approximately the $t_{avg,best}$ value at $L = 4.5\ R_E$. This could indicate the presence of two processes, one with a characteristic time of a few days and which is most prominent at large L-values and one with a characteristic time of around 15 to 20 days. This process is most important at lower L-values but also influences the electron fluxes at higher L.

4. Corrections

In order to improve the correlations we included corrections for the Dst effect and semiannual modulation of the solar wind - magnetosphere coupling and also tested linear combinations of different parameters. There are many possible combinations which could not all be tested. We therefore selected $AP_{18,1}$ and $(V_{sw})_{14,1}$ at $L = 4.5\ R_E$ and $AP_{6,1}$ and $(V_{sw})_{3,1}$ at $L = 6.6\ R_E$ to demonstrate the importance of the different approaches.

4.1. Dst correction

The electron fluxes are influenced by the Dst effect. The magnetic field decrease associated with negative Dst values leads to a deceleration of the electrons and with that to a decrease of the electron fluxes [*McIlwain,* 1966; *Desorgher,* 1999]. In order to take this into account the electron fluxes are multiplied with a factor which is a function of Dst. The tested functions are listed in table 2. Each function has one free parameter, α, which can be fitted to find the best correlation between the corrected electron fluxes and a given geomagnetic/solar wind parameter. The resulting α and corresponding correlation coefficient are given in table 2. The improvements are most significant at $L = 4.5\ R_E$ and less clear at GEO. The difference between the three tested correction functions is negligible.

4.2. Semiannual modulation

The solar wind - magnetosphere coupling strength is a function of the season [*Desorgher et al.,* 1998; *Baker et al.,* 1999]. It is most efficient during spring and fall (equinoxes) and less efficient during summer and winter (solstices). In order to take this into account the solar wind speed is multiplied with a factor which is a function of the season (see table 2) of the three free parameters A, t_0, ω, and the time t which is measured in days. The free parameters can be fitted to find the best correlation between the electron fluxes and the corrected solar wind speed. At $L = 4.5\ R_E$ the semiannual correction yields a significant improvement of the correlation (from non-corrected 0.61 to corrected 0.76), whereas at $L = 6.6\ R_E$ the improvement is small. Altough the two investigated L-values are not conclusive, the results suggest, that the importance of the semiannual modulation decreases with increasing L (lower value of A and less improvement of the correlation at $L = 6.6\ R_E$ compared to $L = 4.5\ R_E$), in agreement with the result found by *Desorgher et al.* [1998]. The fitted parameter values are compatible with t_0=1995-04-21 and $\omega = 0.5$ years.

The same analysis using AP does not yield reasonable results suggesting the modulation in this case to be negligible. This can be expected, since AP itself is affected by the semiannual modulation of the solar-wind-magnetosphere coupling, thus the modulation is already contained in AP [*Joselyn,* 1995].

At low L-values, where the semiannual correction of the solar wind - magnetosphere coupling is important, AP is the better parameter than V_{sw} and at large L-values, where V_{sw} is the best correlating parameter the semiannual correction is small. Thus the correction for the semiannual modulation can not significantly improve the models.

4.3. Linear combination

In section 3 we noted that the $cc_{\mathcal{P}}$ versus t_{avg} curves (see figure 2) suggest two timescales to be important, one of ≈ 5 days and one of ≈ 20 days. The idea here is to use a linear combination of two parameters representing the two different time scales. As an example we selected $AP_{18,1}$ and $(V_{sw})_{3,1}$, the best fitting parameters at $L = 4.5\ R_E$ and GEO. As shown in table 2, using the linear combination does only little improve the correlation.

4.4. Combined corrections

Dst correction, semiannual correction and linear combination of parameters can be combined. But since semiannual correction and linear combination of parameters does not significantly improve the correlation, the combined corrections give similar results as when applying only a Dst correction. The results shown in table 2 were calculated with the Dst correction function $(1 + \alpha \cdot Dst/100)$. Nevertheless, best correlation is found with linear combination of $AP_{18,1}$ and $(V_{sw})_{3,1}$ including a Dst-correction.

5. Flux models

The results of the linear correlation study can be used to select best sorting parameters for simple flux models. Table 3 contains six models at $L = 4.5\ R_E$ and $L = 6.6\ R_E$, which have been determined by a linear fit between the logarithm of the (corrected) 1 MeV electron fluxes and selected (corrected) parameters. Table 3

In figure 3 models 5 & 6 are confronted with the actual measurements. The upper panels show the measured (solid line) and predicted (dotted line) 1 MeV electron fluxes. The lower panels show the relative difference of the logarithm of the fluxes. At $L = 4.5\ R_E$ this difference is within ± 0.2 which means that $f_e^{0.8} \leq f_{model} \leq f_e^{1.2}$. At $L = 6.6\ R_E$ the differences are larger (± 0.4). figure 3

The largest differences occur during the fast flux rises and periods during which the electron densities are very low. Since the fluxes increase with a characteristic time scale of a day, the rises are badly described by the > three-day averages. The rises only occur during a small fraction of the time and therefore have little weight in the correlation coefficient, which is dominated by the longer lasting periods of relatively high and decreasing fluxes.

All of the models have problems to describe the periods with very low electron fluxes. This is especially pronounced at $L = 6.6\ R_E$ where the electron fluxes can continue to dicrease when the driving parameter levels out. An additional term to account for losses could be useful. Possible loss mechanisms are steady losses due to pitch angle scattering, losses during the main phase of magnetic storms due to the outward movement of the trapped particles, or losses from stable trapping due to solar-wind shocks.

6. Conclusions

AP_{15} used by *Brautigam et al.* [1995] to produce the CRRESELE models is indeed a good parameter for sorting the relativistic electron fluxes at the heart of the outer radiation belt. And since the highest electron fluxes are encountered in that region, the models can also be expected to be reliable for estimating the total fluences encountered by a spacecraft in GTO. However, at GEO the timescales of the variations are shorter and using shorter average times and the solar wind velocity instead of AP, gives significantly better correlations.

In this paper we investigated only the 1 MeV electrons. But the variations are also a function of energy and a similar investigation including different energies could be of great interest as input for future modeling efforts.

Acknowledgments. The author would like to thank J. Lemaire for usefull discussions. This work was supported by ESA's Technology Research Program, ESA/TOS-EMA, Space Environments and Effects Major Axis.

References

Baker, D.N., McPherron, R.L., Cayton, T.E., Klebesadel, R.W., Linear prediction filter analysis of relativistic electron properties at 6.6 R_E, *J. Geophys. Res., 95,* 15133, 1990

Baker, D.N., Li, X., Blake, J.B., Kanekal, S., Strong electron acceleration in the earth's magnetosphere, *Adv. Space. Res., 21,* 609, 1998

Baker, D.N., Kanekal, S.G., Pulkinnen, T.I., Blake, J.B., Equinoctial and solstitial averages of magnetospheric relativistic electrons: A strong semiannual modulation, *J. Geophys. Res., 26,* 3193, 1999

Blake, J.B., Baker, D.N., Turner, N., Ogilvie, K.W., Lepping, R.P., Correlation of changes in the outer-zone relativistic-electron population with upstream solar wind and magnetic field measurements, *Geophys. Res. Lett, 24,* 927, 1997.

Bühler, P., Ljungfelt, S., Mchedlishvili, A., Schlumpf, N., Zehnder, A., Adams, L., Daly, E., Nickson, R., Radiation environment monitor, *Nucl. Instr. and Meth. in Phys. Res. A, 368,* 825, 1996.

Brautigam, D.H. and Bell, J.T., CRRESELE Documentation, *Tech. Rep. PL-TR–95-2128,* Phillips Laboratory, Hascom Ait Base, MA 01731-3010, 1995

Desorgher, L., Bühler, P., Zehnder, A., Daly, E., and Adams, L., Outer Radiation belt Variations During 1995, *Adv. Space Res.*, **22**, 83, 1998

Desorgher, L., Variations of the Earth's Outer Radiation Belt, REM Observations between 1995 and 1997 and Simulations of Magnetic Storm Effects, PHD Thesis, University of Bern, Switzerland, 1999

Gonzalez, W.D., Joselyn, J.A., Kamide, Y., Kroehl, H.W., Rostoker, G., Tsurutani, B.T., and Vasyliunas, V.M., *J. Geophys. Res., 99,* 5771, 1994

Joselyn, J.A., Geomagnetic activity forecasting: The state of the art, *Reviews of Geophysics, 33,* 383, 1995

Koons, H.C., Gorney, D.J., and Blake, J.B., Long-Term Variability of Electron Radiation Dose in Geosynchronous Orbit, *J. Spacecraft and Rockets, 31,* 557, 1994

Li, X., Baker, D.N., Temerin, M. et al., Rapid enhancements of relativistic electrons deep in the magnetopshere during May 15, 1997, magnetic storm, *J. Geophys. Res., 104,* 4467, 1999

McIlwain, C.E., Ring current effects on trapped particles, *J. Geophys. Res., 71,* 3623, 1966

Nagai, T., Space weather forecast: Prediction of relativistic electron densities at synchrounous orbit, *Geophys. Res. Lett., 15,* 425, 1988

NGDC, NOAA National Data Centers at http:www.ngdc.noaa.govsegpotfldgeomag.shtml

Paulikas, G.A. and Blake, J.B., Effects of the solar wind on magnetospheric dynamics: energetic electrons at the synchronous orbit, in *Quantitative modeling of magnetospheric processes*, edited by W. P. Olson, Geophysical Monograph Series 21, 181, 1979

WIND, WIND information at http:nssdc.gsfc.nasa.govspaceistpwind.html

Vette, J.I., The AE8 trapped electron model environment., *Tech. Rep. NSSDC WDC-A-R&S, 91-24,* NASA–GSFC, 1991

Wrenn, G. and Smith, R., The ESD threat to GEO satellites: empirical models for observed effects due to both surface and internal charging, *Proc. ESA Symposium on Environment Modelling for Space-based Applications, SP-392,* 121, 1996

P. Bühler, L. Desorgher, A. Zehnder., Laboratory for Astrophysics, Paul Scherrer Institute, 5232 Villigen, PSI, Switzerland (e-mail: paul.buehler@psi.ch; laurent.desorgher@phim.unibe.ch; alex.zehnder@psi.ch)

M. Kruglanski, B. Quaghebeur, Belgian Institute for Space Aeronomy, 1180 Brussels, Belgium (e-mail: michelk@mail.magnet.oma.be; bart.quaghebeur@bira-iasb.oma.be)

E. Daly, ESTEC, NL-2200 AG Noordwijk, The Netherlands (e-mail: eamonn@wm.estec.esa.nl)

This preprint was prepared with AGU's LaTeX macros v5.01. File corr˙paper formatted February 29, 2000.

Figure 1. 1 MeV electron fluxes at a) $L = 4.5\ R_E$ and b) 6.6 R_E measured with REM aboard Strv-1b. Compared with $L = 4.5\ R_E$, the relative flux variations at GEO are larger and obviously have a shorter characteristic time scale.

Figure 2. Correlation coefficient cc_{AP} (left panels) and $cc_{V_{sw}}$ (right panels). Panels a) and c) show greyscale coded L-t_{avg}-maps of the correlation coefficients. The black dots mark the positions where the correlation is maximum at a given L-bin. The panels below show the maximum correlation coefficient at a given L-bin as function of L. In panels b) and d) the correlation coefficients at $L = 4.5\ R_E$ (diamonds) and $L = 6.6\ R_E$ (astrisks) are plotted versus t_{avg}.

Figure 3. Flux model results for a) model 5 (see table 3) and b) model 6. In the upper panels the measured (solid line) and predicted (dotted line) 1 MeV electron fluxes are plotted versus time. The lower panels show the relative difference between the logarithms of the measured and predicted fluxes. Model fluxes for which this difference is larger than 0.2 are marked with red, such for which the difference is lower than -0.2, are marked with blue.

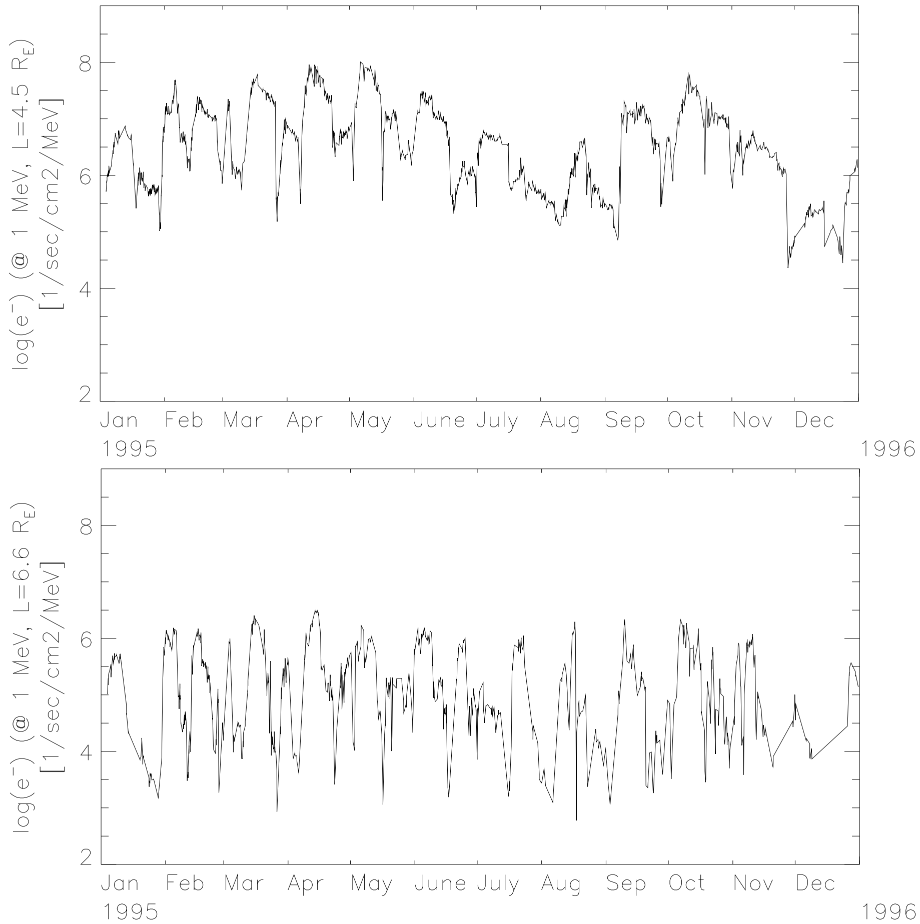
log(e⁻) (@ 1 MeV, L=4.5 R_E)
[1/sec/cm2/MeV]
2
4
6
8
Jan
Feb
Mar
Apr
May
June
July
Aug
Sep
Oct
Nov
Dec
1995
1996
log(e⁻) (@ 1 MeV, L=6.6 R_E)
[1/sec/cm2/MeV]
2
4
6
8
Jan
Feb
Mar
Apr
May
June
July
Aug
Sep
Oct
Nov
Dec
1995
1996

a)

b)

Figure 1.

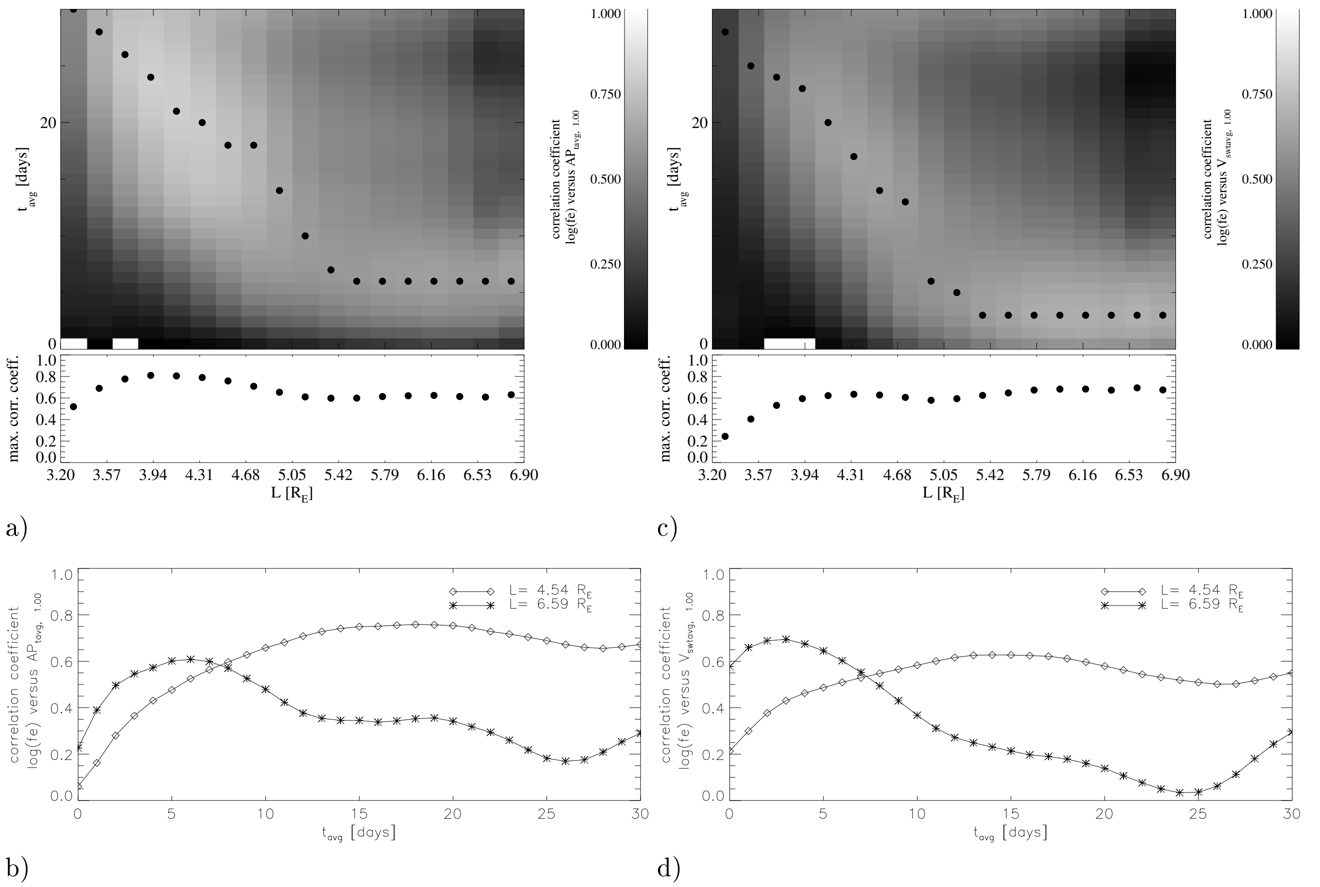
t avg [days]
correlation coefficient log(fe) versus AP tavg, 1.00
max. corr. coeff.
L [R_E]
a)
correlation coefficient log(fe) versus V swtavg, 1.00
c)
L= 4.54 R_E
L= 6.59 R_E
t avg [days]
b)
d)

Figure 2.

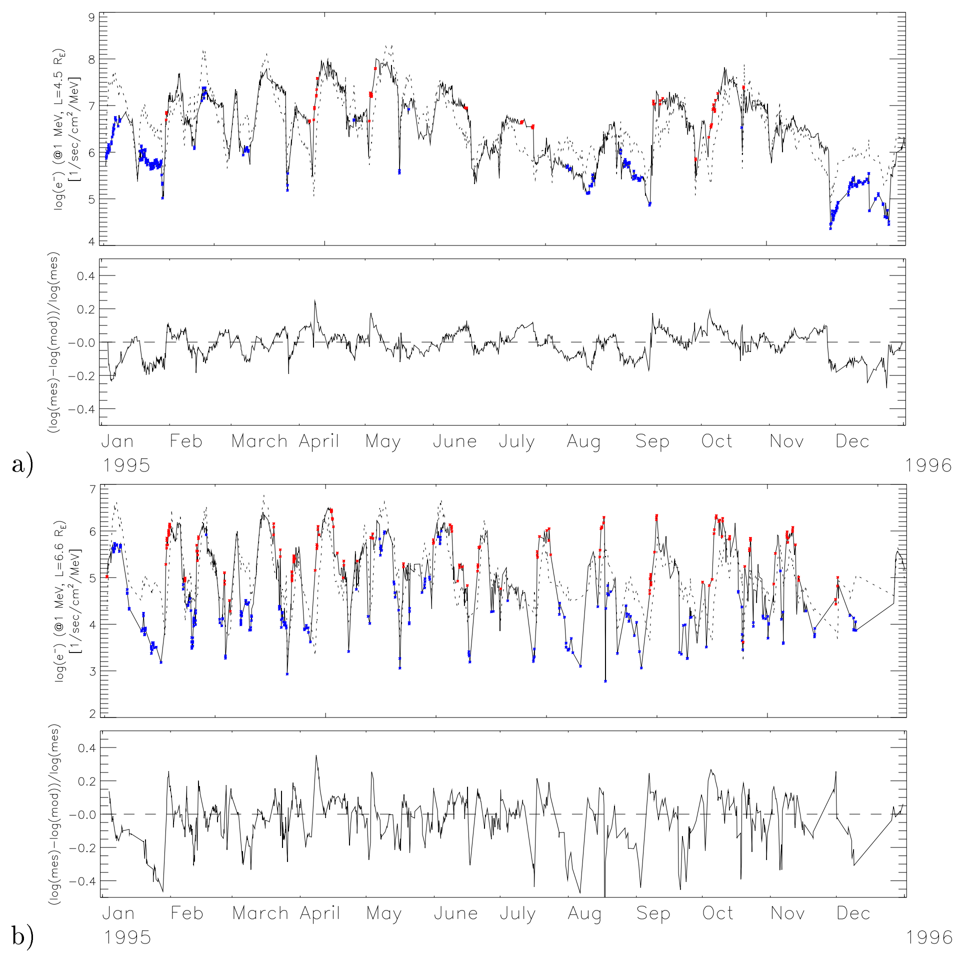
log(e⁻) (@1 MeV, L=4.5 R$_E$) [1/sec/cm^2/MeV]
(log(mes)−log(mod))/log(mes)
Jan Feb March April May June July Aug Sep Oct Nov Dec
1995
1996
a)
log(e⁻) (@1 MeV, L=6.6 R$_E$) [1/sec/cm^2/MeV]
(log(mes)−log(mod))/log(mes)
Jan Feb March April May June July Aug Sep Oct Nov Dec
1995
1996
b)

Figure 3.

Table 1. Parameter functions used to study correlation with 1 MeV electron fluxes. The right four columns contain $t_{avg,best}$ and corresponding $cc_{\mathcal{P},best}$ at $L = 4.5\ R_E$ and $L = 6.6\ R_E$ (see text for details).

Function	$t_{avg,best}$ [days]		$cc_{\mathcal{P},best}$	
	4.5 R_E	6.6 R_E	4.5 R_E	6.6 R_E
AP	18	6	0.76	0.61
aa	19	6	0.73	0.61
Dst	18	2	0.68	0.46
V_{sw}	14	3	0.63	0.69
$V_{sw}B_{imf,z}$	6	5	0.26	0.38
$V_{sw}B_{imf,s}{}^{(1)}$	21	5	0.53	0.33
$V_{sw}B_{imf,t}{}^{(2)}$	19	8	0.58	0.42
$V_{sw}^2 B_{imf,z}$	7	5	0.32	0.36
$V_{sw}^2 B_{imf,s}$	20	5	0.64	0.51
$V_{sw}B_{imf,t}sin(\Theta/2)^{(3)}$	20	7	0.59	0.49
$V_{sw}B_{imf,t}sin^2(\Theta/2)$	20	6	0.58	0.50
$V_{sw}B_{imf,t}sin^4(\Theta/2)$	20	6	0.58	0.48
$(\rho V_{sw}^2)^{1/2} V_{sw} B_{imf,z}$	21	5	0.28	0.35
$(\rho V_{sw}^2)^{-1/3} V_{sw} B_{imf,t}^2 sin^4(\Theta/2)$	21	22	0.39	0.24
$(\rho V_{sw}^2)^{1/6} V_{sw} B_{imf,t} sin^4(\Theta/2)$	21	7	0.61	0.50
$\epsilon = V_{sw} L_0^2 B_{imf}^2 sin^4(\Theta/2)^{(4)}$	21	8	0.66	0.52

$^{(1)}$ $B_{imf,s} = \begin{cases} B_{imf,z} & : \quad B_{imf,z} > 0 \\ 0 & : \quad B_{imf,z} \leq 0 \end{cases}$

$^{(2)}$ $B_{imf,t}^2 = B_{imf,y}^2 + B_{imf,z}^2$

$^{(3)}$ Θ is the clock angle between $B_{imf,z}$ and the IMF vector projected at the magnetopause ($[B_{imf,y},\ B_{imf,z}]$)

$^{(4)}$ L_0 is a constant scale-length factor, equal to 7 R_E

Table 2. Correction functions, best fitting parameters, and corresponding linear correlation coefficients.

Correction function		correlation coefficient $L = 4.5\ R_E$		correlation coefficient $L = 6.6\ R_E$	
No correction		$AP_{18,1}$	$(V_{sw})_{14,1}$	$AP_{6,1}$	$(V_{sw})_{3,1}$
		0.76	**0.61**	**0.63**	**0.69**
Dst correction					
$exp(\alpha \cdot Dst/100)$		**0.83**	**0.73**	**0.64**	**0.72**
	$\alpha =$	-0.209	-0.027	-0.589	-0.290
$1 + \alpha \cdot Dst/100$		**0.83**	**0.74**	**0.64**	**0.72**
	$\alpha =$	-0.225	-0.027	-0.743	-0.337
$(1+\alpha)^{(-Dst/100)}$		**0.83**	**0.73**	**0.64**	**0.72**
	$\alpha =$	0.233	0.027	0.802	0.336
Semiannual correction					
$1. + A \cdot cos(2\pi(t_0 - t)/\omega)$					
		-	**0.76**	-	**0.70**
	$A =$		0.122		0.056
$t_0 \approx$ 1995-04-21					
$\omega \approx 0.5$ years					
Linear combination					
$\frac{AP_{18,1}}{max(AP_{18,1})} + \beta \cdot \frac{(V_{sw})_{3,1}}{max((V_{sw})_{3,1})}$					
$max(AP_{18,1}) = 22.69$, $max((V_{sw})_{3,1}) = 700.0$					
		0.79		**0.71**	
	$\beta =$	0.176		4.87	
Linear combination with Dst correction					
		0.84		**0.75**	
	$\alpha =$	-0.253		-0.412	
	$\beta =$	0.283		3.67	

Table 3. 1 MeV electron flux models for $L = 4.5\ R_E$ and GEO.

Model		$log10(f_e) =$
1	$L = 4.5\ R_E$	$4.67 + 0.145 \cdot AP_{18,1}$
2	$L = 6.6\ R_E$	$2.52 + 5.73 \cdot 10^{-3} \cdot (V_{sw})_{3,1}$
3	$L = 4.5\ R_E$	$(4.57 + 0.167 \cdot AP_{18,1})/(1 - 2.25 \cdot 10^{-3} \cdot Dst_{0,0})$
4	$L = 6.6\ R_E$	$(2.25 + 6.88 \cdot 10^{-3} \cdot (V_{sw})_{3,1})/(1 - 3.37 \cdot 10^{-3} \cdot Dst_{0,0})$
5	$L = 4.5\ R_E$	$(4.11 + 1.57 \cdot 10^{-1} \cdot (AP_{18,1} + 9.17 \cdot 10^{-3} \cdot (V_{sw})_{3,1}))/(1 - 2.53 \cdot 10^{-3} \cdot Dst_{0,0})$
6	$L = 6.6\ R_E$	$(1.70 + 5.47 \cdot 10^{-2} \cdot (AP_{18,1} + 1.19 \cdot 10^{-1} \cdot (V_{sw})_{3,1}))/(1 - 4.12 \cdot 10^{-3} \cdot Dst_{0,0})$